Numerical simulation of solar radiation, air flow and temperature distribution in a naturally ventilated tunnel greenhouse

Catherine Baxevanou[1], Dimitrios Fidaros[1], Thomas Bartzanas[1], Constantinos Kittas[1,2]*

([1]Center for Research and Technology-Thessaly, Institute of Technology and Management of Agricultural Ecosystems, Technology Park of Thessaly, 1st Industrial Area, 38500 Volos; [2]University of Thessaly, Department of Agriculture, Crop Production and Agricultural Environment, Fytokou St., N. Ionia, GR-38446, Magnesia, Greece)

Abstract: The effect of solar radiation distribution in a typical agricultural building was numerically investigated, taking into account the thickness of the cover, its spectral optical and thermal properties. A two dimensional mesh was used to render the building's geometry, and the Discrete Ordinate (DO) model for simulating the radiation, taking into accounts its spectral distribution in three wavelength bands. Based on the meteorological data of October for the region of Volos (Greece), two parametric studies were carried out, dealing with the variation of intensity and angle of the incoming solar radiation and with the optical properties differentiation of covering materials. The flow recirculation, due to the buoyancy effect, showed the importance of internal temperature gradients, although forced convection which resulted from natural ventilation was dominant. It was concluded that cover material with high absorptivity deteriorate the natural ventilation increasing the air temperature by convection, and favoring the development of secondary recirculation where the air is trapped. Furthermore, high absorptivity reduces the available Photosynthetically Active Radiation (PAR) but it distributes it equally inside the greenhouse. Finally, the ability of the material to transmit the solar irradiance in the wavelengths corresponding to PAR with comparable absorptivity improved as the refractive index decreased.

Keywords: greenhouse, microclimate, CFD, radiation, mixed heat transfer, ventilation, Greece

1. Introduction

Worldwide agricultural production under controlled environments has increased steadily in recent years. Controlled environment agriculture systems offer the opportunity to modify the indoor climate and to create an environment that is optimal for growth and production, both in terms of quality and quantity. Greenhouse cultivations constitute the most productive form of primary agricultural production. In those structures, indoor climate conditioning is a tool to improve the growing conditions, allowing higher yields and better quality compared with outdoor growing conditions. Knowledge of radiation distribution is important since it is the main input and driving force for many physiological functions and energy transfers.

The most important factor affecting plant growth and development, in greenhouses, is solar radiation since, apart from its indirect effect on greenhouse air temperature, it governs two important physiological mechanisms of the plants, namely transpiration and photosynthesis. The amount of solar radiation entering the greenhouse is highly dependent on greenhouse design, thermo-physical and optical properties of the covering material, and weather conditions.

Information not only about the quantity and quality, but also about the spatial distribution of daylight transmitted by greenhouse cladding or shading materials is essential to a further evaluation of their influence on the growth and development of plants. From a quantitative point of view, the amount of solar energy transmitted into the greenhouse drives the physiological activity. Transpiration is dependent on the quantity of solar radiation incident on the canopy, and photosynthesis is dependent on the quantity of PAR (photosynthetic active

radiation, 400-700 nm) absorbed by the canopy, thus determining the global productivity of the crop (Monteith, 1977; Cockshull, Graves and Cave, 1992). From a qualitative point of view, the spectrum of the outside solar radiation can be significantly modified by the optical properties of the greenhouse cover. These qualitative changes in the radiation transmitted inside the greenhouse induce morphogenetic effects and can result in modifications of the architecture and shape of the plants with significant consequences, in some cases, on the value of the crop, especially ornamental crops. The amount of energy absorbed by the crop for photosynthesis can be ignored in the crop energy balance. Therefore, almost all solar energy entering the greenhouse is absorbed as thermal energy by the crop and by the rest of the greenhouse parts including its soil. A portion is released by the crop transpiration, as latent heat, and the rest contributes to the sensible heat balance of the total greenhouse system. For north European climatic conditions, it estimated that solar energy contributes about 50% of the yearly heat demand of a single glass greenhouse; input from fossil energy has to contribute the other 50%.

One of the most important aspects in greenhouse climate conditioning is its spatial distribution. Radiative heterogeneity is particularly important in tunnel greenhouses, the most commonly used greenhouse type in the Mediterranean basin. This variability severely affects plant activity and often leads growers to over fertilize their crop, as it has been observed for lettuce crops (De Tourdonnet, 1998). The differences on climate distribution not only cause non-uniform production and quality, but also cause problems with pests and diseases. If climate distribution can be predicted in a more precise way, energy can be saved and pressure of pests and diseases is decreased, enabling pest and disease control in a more sustainable way, e.g. biologically. Knowledge of climate distribution and variation should help to improve its homogeneity by modifying the design of the greenhouse structure and climate air conditioning systems and by locally controlling these systems. This requires the characterisation and modelling of the processes, particularly of convective heat transfers, involved in its elaboration (Boulard and Wang, 2002).

An approximate model (Rosa, Silva and Miguel, 1989) has been developed for single-span semicircular greenhouses, which assumes that all incident radiation (Duffie and Beckman, 1980) is isotropically scattered on the cladding. Also, other models were developed (Kurata, Quan and Nunomura, 1991; Critten, 1993; Papadakis, Manolakos and Kyritsis, 1998) with simple shape optimisation for single-span tunnels, however, they took into account only direct-beam radiation, while failing to allow for the scattering of incident radiation by the cladding. Diffuse light transmissivity was taken as the average of direct light transmissivity from different parts of the sky vault. In other words, all incident radiation is assumed to be direct and to remain so, even after it has passed the cladding. These models are, therefore, suited only for glass houses and not for plastic greenhouses, since such covering materials (plastics) scatter most of the incoming radiation towards the inner part of the greenhouse. Only internal reflection is taken into account. Using such a model (Kurata, 1990), it was found that the best direction of the greenhouse is the East –West (EW) orientation. In a later work (Kurata, Quan and Nunomura, 1991), the optimal shape from the point of view of radiation was determined for the single-span greenhouse with straight cladding. It should be mentioned that for all these models, accurate values for the transmission coefficient of the cover are needed. Takakura (1993) studied the change in radiation as a function of time on a horizontal surface. A simple model was developed to calculate the transmission of greenhouse glass cladding as a function of incident angle. Transmission and reflection for glass planes were also measured (De Zwart, 1993) as a function of angle of incidence. The change in transmission caused by condensation on the cladding materials was studied by Pollet et al. (1999).

The radiative heterogeneity at the greenhouse floor level (Wang and Boulard, 2000) was simulated as a function of greenhouse geometry, covering material and weather conditions. More recently, a computational algorithm has been presented (Vougioukas, 2004), which computes the light distribution on any greenhouse surface based on a global radiation transfer model, such as the ones that have been developed for computer graphics applications. The particular algorithm solves numerically the integral light transport equation, which relates radiance, environment geometry and optical surface characteristics for diffuse environments of arbitrary complexity.

Most of the above mentioned studies for computing greenhouse solar transmissivity are analytical and cannot handle the combined effects of light scattering due to cladding, multiple reflections of diffuse light, and complex non-planar geometries, such as the ones found in multi-span tunnels of variable roof cross-section. Moreover, no detailed information was provided about the influence of the solar radiation distribution on the energy balance of the greenhouse. In recent years the use of computational fluid dynamics enables easier studies of scalar and vector variables which determines greenhouse microclimate with respect to its structural specifications and used equipment (Boulard and Wang, 2002; Bartzanas, Boulard and Kittas, 2004; Fatnassi et al., 2006; Ould Khaoua et al., 2006). However, in those studies radiation was not simulated directly through a radiative transfer equation but its effect was indirectly incorporated in their models either in the formation of boundary conditions or as an extra source term in energy transport equation.

In the present study, a commercially available computational fluid dynamics code was used to investigate the distribution of solar radiation in a naturally ventilated arc type tunnel greenhouse and its influence on greenhouse microclimate, taking into account the external incident radiation distributed in three wavelength bands and the spectral optical properties of the involved materials. Two parametric studies were performed studying six cover materials with various optical properties and five incident angles of solar radiation.

2. Materials and methods

2.1. The mathematical model

The flow inside the greenhouse is assumed to be two dimensional (2D), steady-state, incompressible and turbulent (Ferziger and Peric, 2002). Although 2D simulation does not render precisely the reality inside the greenhouse, it could be a computationally beneficial assumption for the investigation of the transport phenomena especially at the middle section of a long structure with side opened vents along the whole length.

The present flow and transport phenomena for air flow and the heat transfer are described by the Navier-Stokes equations. The time-averaged Navier-Stokes equations, for the momentum, mass and energy transport are given as follow:

$$\text{Continuity equation} \quad \frac{\partial U_i}{\partial x_i} = 0 \tag{1}$$

$$\text{Momentum conservation} \quad \rho U_j \frac{\partial U_i}{\partial x_j} = -\frac{\partial P}{\partial x_i} + \frac{\partial}{\partial x_j}\left[(\mu + \mu_t) \frac{\partial U_i}{\partial x_j} \right] + f_b + S_i \tag{2}$$

The density variation was calculated according to the Boussinesq model in order to take into account the natural convection effects (Gray and Giorgini, 1976). The crop was simulated using the equivalent porous medium approach (Boulard and Wang, 2002) by the addition of a momentum source term, due to the drag effect of the crop, to the standard fluid flow equations. The equivalent macro-porous medium refers to the combination of the porous medium approach (to model the dynamic effect of the crop cover on the flow) with a macro-model of heat and mass transfer between the leaves and air within each mesh of the crop cover. The crop aerodynamic resistance was determined from the laminar boundary layer theory using the computed air velocity in each node of the crop volume mesh, and the

stomatal resistance was considered as a function of both the global radiation density and the vapor pressure deficit. A detailed description of equations used to describe the crop resistance to the air flow and the heat and mass exchanges between crop and air can be found in Bartzanas, Boulard and Kittas (2004).

The effect of turbulence on the flow was implemented via the high Re k-ε model (standard) model (Launder and Spalding, 1972). The standard k-ε model is a semi-empirical model based on model transport equations for the turbulent kinetic energy (k) and its dissipation rate (ε). The complete set of the equations of the *k-ε* model can be found in Mohammadi and Pironneau (1994) and their commonly used set of parameters (empirically determined) are $C_\mu = 0.09$, $\sigma_\kappa = 1$, $C_{\varepsilon 1} = 1.44$, $C_{\varepsilon 2} = 1.96$, and $\sigma_\varepsilon = 1.3$ (Fluent, 1998)

The computation of energy distribution at the interior of the greenhouse and at the solid part of its covering is the general transport convection-diffusion equation in terms of enthalpy and taking into account the viscous dissipation

$$\text{Energy Conservation } \rho\left(U_i \frac{\partial h}{\partial x_i}\right) = \frac{\partial}{\partial x_i}\left(k_{eff} \frac{\partial T}{\partial x_i}\right) + S_h \tag{3}$$

Auxiliary relationships for the calculations of quantities which appear in energy equation are presented here. In particular, relationships are given for the calculation of effective and turbulent conductivity, as well as for the energy and enthalpy. The energy equation is also solved in solid regions where it is reduced to a Laplacian operator (Fluent, 1998). The energy balance inside the greenhouse incorporates the effect of radiation as source term in energy equation which is taken by the solution of the radiative transport equation.

2.2. Radiation modelling

In order to simulate the effect of solar incident radiation on the greenhouse cover the Discrete Ordinate DO model is used. In this model it was assumed that radiation energy was 'convected' simultaneously in all directions through the medium at its own speed. The DO model allows the solution of radiation at semi-transparent walls. It can be used to non-gray radiation using a gray-band model. So it is adequate for use with participating media with a spectral absorption coefficient α_λ that varies in a stepwise fashion across spectral bands.

The discrete ordinates (DO) radiation model solve the Radiative transfer equation (RTE) for a finite number of discrete solid angles, each associated with a vector direction $\vec{s}$ fixed in the global Cartesian system (x,y,z). It transforms the RTE equation into a transport equation for radiation intensity in the spatial coordinates (x,y,z). The DO model solves for as many transport equations as there are directions $\vec{s}$ (Raithby and Chui, 1990; Chui and Raithby, 1993). The RTE for spectral intensity $I_\lambda\left(\vec{r},\vec{s}\right)$ turns to

$$\nabla\left(I_\lambda\left(\vec{r},\vec{s}\right)\vec{s}\right) + \left(\alpha_\lambda + \sigma_s\right)I_\lambda\left(\vec{r},\vec{s}\right) = \alpha_\lambda n^2 I_{b\lambda}\left(\vec{r}\right) + \frac{\sigma_s}{4\pi}\int_0^{4\pi} I_\lambda\left(\vec{r},\vec{s}'\right)\Phi\left(\vec{s}\cdot\vec{s}'\right)d\Omega' \tag{4}$$

In this equation the refractive index, the scattering coefficient and phase function are assumed independent of wavelength. The phase function Φ, is considered isotropic. The angular space 4π at any spatial location is discretized into $N_\theta \times N_\varphi$ solid angles of extent ω_i, called control angles. The angles θ and φ are the polar and azimuthal angles, and are measured with respect to the global Cartesian system (x,y,z). In our case a 3x3 pixilation is used. Although in this equation the refraction index is considered to be constant, in the calculation of black body emission as well as in the calculation of boundary conditions imposed by semi-transparent walls the band length depended values of refractive index are used. This angular discretization provides us with a moderate computational cost but it may introduce discretization errors at boundaries when the solid angles are bisected by the boundaries (Raithby, 1999). Solving a problem with a fine angular discretization may be CPU-intensive.

The RTE equation is integrated over each wavelength. Then the total intensity $I(\vec{r}, \vec{s})$ in each direction $\vec{s}$ at position $\vec{r}$ is computed using

$$I(\vec{r}, \vec{s}) = \sum_\kappa I_{\lambda_\kappa}(\vec{r}, \vec{s}) \Delta\lambda_\kappa \tag{5}$$

where the summation is over the wavelength bands.

The RTE equation is coupled with the energy equation through a volumetric source term given by the following equation (Kim & Huh, 1999):

$$S_h = -\frac{\partial q_{r_i}}{\partial x_i} = \alpha_\lambda \left(4\pi I_{b\lambda}(\vec{r}) - \int_{4\pi} I(\vec{r}, \vec{s}) d\Omega \right) \tag{6}$$

The spectral absorption coefficient, α_λ, (or extinction coefficient) is computed from the absortpivity, α, from the following relationship, according to the media thickness, d:

$$\alpha_\lambda = \frac{1}{d} \ln\left(\frac{1}{1-\alpha}\right) \tag{7}$$

2.3. Numerical details

The commercial CFD code Fluent (Fluent, 1998) was used for the computations, where external source code was embodied for the boundary conditions (written in C). The integration of radiative transfer equation (RTE) was described by the study of (Murthy Mathur, 1998). Equations are resolved numerically by finite volume method, using a two dimensional structured mesh consisted of 20.000 cells. The SIMPLE (Patankar, 1980) algorithm is used for pressure-velocity coupling, yielding an elliptic differential equation in order to formulate the mass conservation equation. The discretisation of the convective terms in the Reynolds averaged transport equations is materialized by the SOU scheme (Tamamidis and Assanis, 1993) and for the diffusive terms a central difference scheme is adopted. The convergence criterion was set to 10^{-7} for the continuity, momentum and turbulence equations, while for energy and radiation equation the criterion was 10^{-8}.

2.4. Boundary conditions

The reference case study concerns a typical low cost Mediterranean arc type tunnel greenhouse. The geometrical characteristics of the tested greenhouse were as follows: eaves height = 2.4 m; ridge height = 4.1 m; total width = 8 m; total length = 20 m; ground area A_g = 160 m^2, and volume V = 572 m^3. The greenhouse was equipped with two side continuous roll-up vents located at a height of 0.65 m above the ground with a maximum opening area of 13.5 m^2 (15 m length × 0.9 m height) for each one (Figure 1).
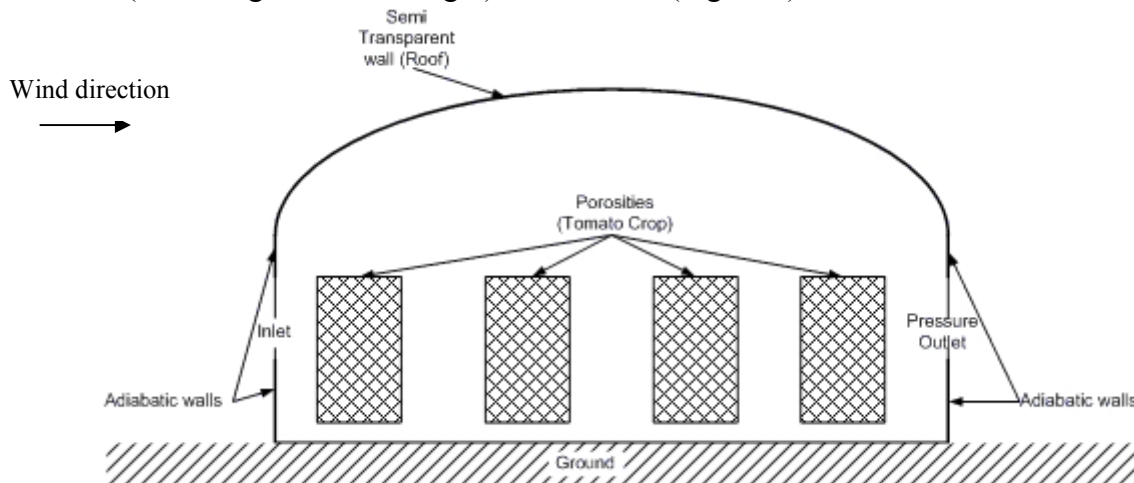

Figure 1 Flow geometry for the tunnel-arc greenhouse

From the left opening, which is supposed to face the East, air enters with a given velocity profile (Figure 2) preserving turbulent intensity 3% and temperature 289.2 K, which is considered to be the temperature of ambient air around the greenhouse. This geometry allows a 2D approach without introducing major errors for the study of section close to the middle. The inlet is considered a fully developed turbulent profile, following power law (Deshpande and Giddens, 1980) for the streamwise velocity. The right opening (leeward) was considered a constant pressure (P=P$_{atm}$) outlet boundary. The cover was considered as a finite thickness wall consisted of semi-transparent materials.
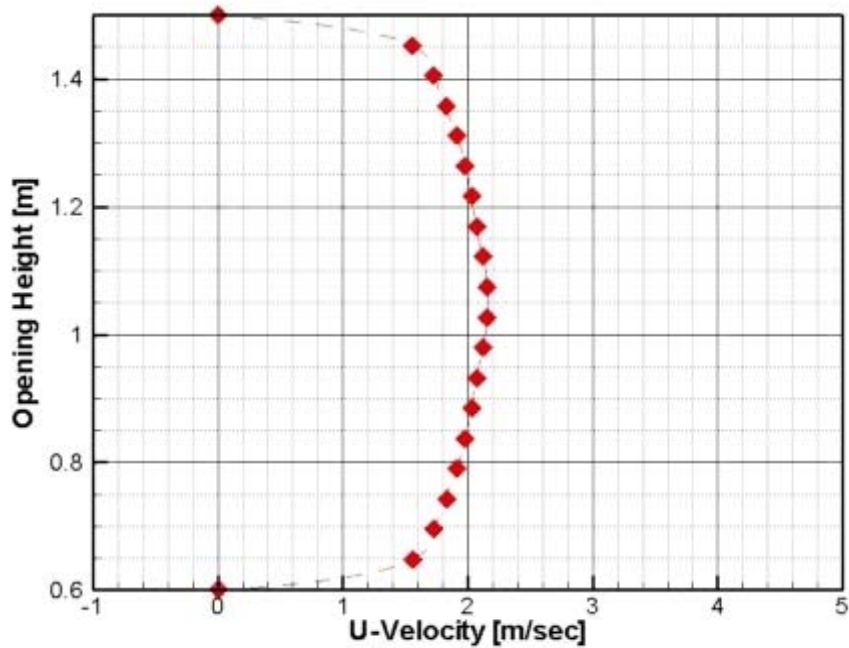

Figure 2 Inlet profile for the streamwise velocity

As far as the cover is concerned, since the solid zone thickness is considered to be 1 cm, for reasons of grid construction simplicity, the optical and thermal properties are modified appropriately in order to take into account the real cover thickness. The cover is a solid zone composed by 4 rows of cells where the conduction thermal equation is being solved (Figure 3). A mixed heat transfer boundary condition (combination of radiation and convection with convective heat transfer coefficient, h=8.3 W/m^{2}K) is applied at the external boundary of the solid region. Also, the same boundary condition is imposed at the internal margin where the solid and the fluid zones are coupled, restoring a conjugated heat transfer treatment at the specific area. The side walls are considered adiabatic and opaque while the ground is considered a diffusively radiating opaque material.
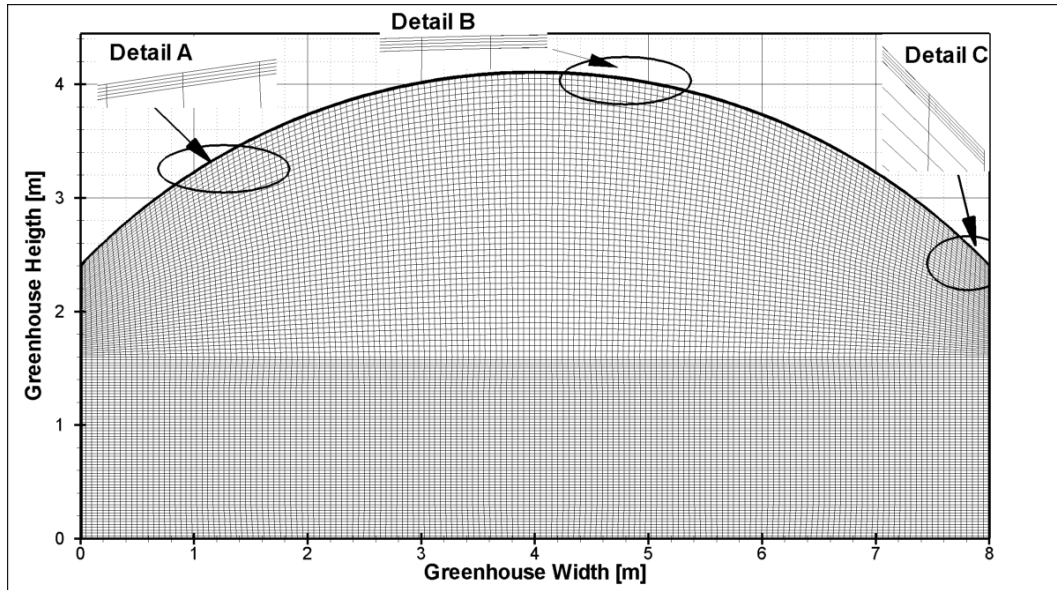
Figure 3 Computational grid of 20000 cells with detailed views of the cover

The plants are simulated as porous materials with viscous resistance $\left(\frac{1}{a}\right)$=27380 [1/m^2] and inertial resistance C_2=1.534[1/m]. The thermal properties of the plants are taken into account through the effective value of the heat transfer coefficient, concerning volume percentage of solid material to be the 60% of the total plant volume, while the optical properties are taken into account only as far as the PAR band is concerned (Pieters & Deltour, 1997). The parameters used in pressure drop expression for the tomato cultivation are derived by (Molina-Aiz et al. 2006) for a low velocity range. For the porous media calculations wood is considered as participating solid material. Table 1 presents the optical properties of the involved materials which are used and in the Table 2 the thermal properties. Internal air optical properties are defined by the high content of evaporated H_2O, while for the setup of boundary conditions, the ambient air emissivity outside of the computational domain is considered to be ε_{ext}=0.05.

Table 1 Material optical properties (Pieters and Deltour, 1997)

Material	Absorptivity, α	Scattering coefficient, σ_s	Refractive index, n	Emissivity
Cover	Wavelength band depended (Material 2 of Table 4)	0	Wavelength band depended (material 2 of table 3)	0.7
Side	Wavelength band depended (Material 2 of Table 4)	0	Wavelength band depended (material 2 of table 3)	0.7
Ground	0.9	-10	1.92	0.95
Crop	0.46	0	2.77	0.46
Air	0.19	0	1	0.9

Table 2 Material thermal properties

Material	Density, ρ [Kg/m^3]	Heat transfer conduction coefficient, k [W/mK]	Specific Heat Capacity, C_p [J/kgK]
Cover	923	0.38	2300
Side	923	0.38	2300
Ground	1300	1.00	800
Crop	700	0.173	2310
Air	1.225	0.0242	1006.43

Experimental results for the examined problem are not available in the relative literature, but simulations studies like present one may serve as a guide for configuration of future experiments.

2.5. Parametric studies

Two parametric studies were carried out in order to investigate the effect of thermal buoyancy in the flow and temperature pattern of the greenhouse, as well as the effect of different cover materials with different optical characteristics.

For the first parametric study a typical day of October was chosen for a greenhouse sited in the region of Volos (Greece), and five hour angles were studied. In each hour angle not only the direction but also the magnitude of solar irradiance varies (Duffie and Beckman, 1980). The incident irradiance is distributed in three wave length bands. The ultra-violet (λ=0.01 – 0.4 μm), the visible or PAR (λ=0.4 – 0.76μm) and the near infrared (λ=0.76-1.1 μm). In Table 3 the normal irradiance per wavelength band are presented. In all cases a fraction of 24% diffuse radiation was considered.

Table 3 Hour angle parametric study

Case	Solar Irradiance [W/m^2]			Hour angle [^{o}]
	UV	PAR	NIR	
Case1	16.56	132.5	116	-60
Case2 - reference	33.75	270	236	-30
Case3	40	320	280	0
Case4	33.75	270	236	30
Case5	16.56	132.5	116	60

For the second parametric study, seven cover materials with different optical properties where studied for the same day of October and for an hour angle of -30°. The used spectral optical properties are given in Table 4. It should be noted that for the parametric study of hour angle the properties of the Material 2 of the Table 4 was used (Kittas & Baille, 1998).

Table 4 Optical properties of used materials

Case	Material name	Absorptivity, α			Refractive index, n		
		UV	PAR	NIR	UV	PAR	NIR
Material 1	Glas sample (GL) – (d= 4mm]	0.05	0.1	0.2	1.65	1.65	1.72
Material 2 (Reference case)	Low density polyethylene film (LDPE) – (d=0.1 mm)	0.37	0.09	0.05	1.72	1.79	1.79
Material 3	Thermal polyethylene film (TPE) – (d= 1 mm)	0.24	0.08	0.06	1.79	1.86	1.86
Material 4	Bubbled polyethylene plastic film (BPE) – (d=0.1 mm)	0.29	0.23	0.18	2.13	2.2	2.2
Material 5	Ethylene vinyl acetate	0.02	0.03	0.04	1.86	1.79	1.72

	film (EVA) – (d=0.15 mm)						
Material 6	Three-layer co-extruded film (3L) – (d=0.45 mm)	0.08	0.06	0.05	1.86	1.79	1.72
Material 7	Rose Polyvinylchloride-based fluorescent (FPVC) – (d=0.15 mm)	0.40	0.52	0.16	1.79	1.79	1.92

3. Results and discussion

Indicative results concerning the first parametric study are presented in Figures 4-10 in terms of flow streamlines, air temperature and PAR radiation contours for all cases. Also, profiles of velocity, temperature and PAR radiation at specific sections are given followed by distributions of radiation heat flux and Nusselt, Bolztmann and Stark numbers.

3.1 Influence of hour angle

3.1.1. Flow field

In Figure 4 the flow streamlines of all cases concerning the first parametric study (a-e) are presented in addition to the simple consideration of pure convective flow without taking into account the radiation effects (f). The flow is dominated by the strong convection of the incoming air through the windward opening. The flow is damped by plants (porosities) and is separated into two unequal streams. The main strong stream, flows at upper part of the plants and the small one flows under them with lower speed. The flow velocities inside the porous regions are decelerated by the viscous and inertial resistance. Three recirculation patterns are observed in the examined field. Two of them appear at the top and bottom corner of the inlet, trapping small amounts of fluid. The recirculation formed at the bottom corner near the entrance seems to be independent of radiation. On the contrary, the existence of the upper corner recirculation is due to radiation effects. When radiation is neglected, the recirculation disappears. Its size is determined by the combination of solar radiation and the direction of the main flow in the greenhouse. During the morning hours, when the solar radiation direction coincides with the entering air stream, it covers a small area, which is extended, proceeding to the solar noon where it presents maximum. The size of the recirculation is decreased till to the total disappearance while the sun is setting. The third recirculation is located between the cover and the main stream flow. It plays significant role in the total flow pattern and the temperature distribution (as it will be shown later), since it divides the domain in two distinguished areas. The extensive area of the specific recirculation is due to the 2D approach, which corresponds to a greenhouse with fully opened continuous vents along the side wall.
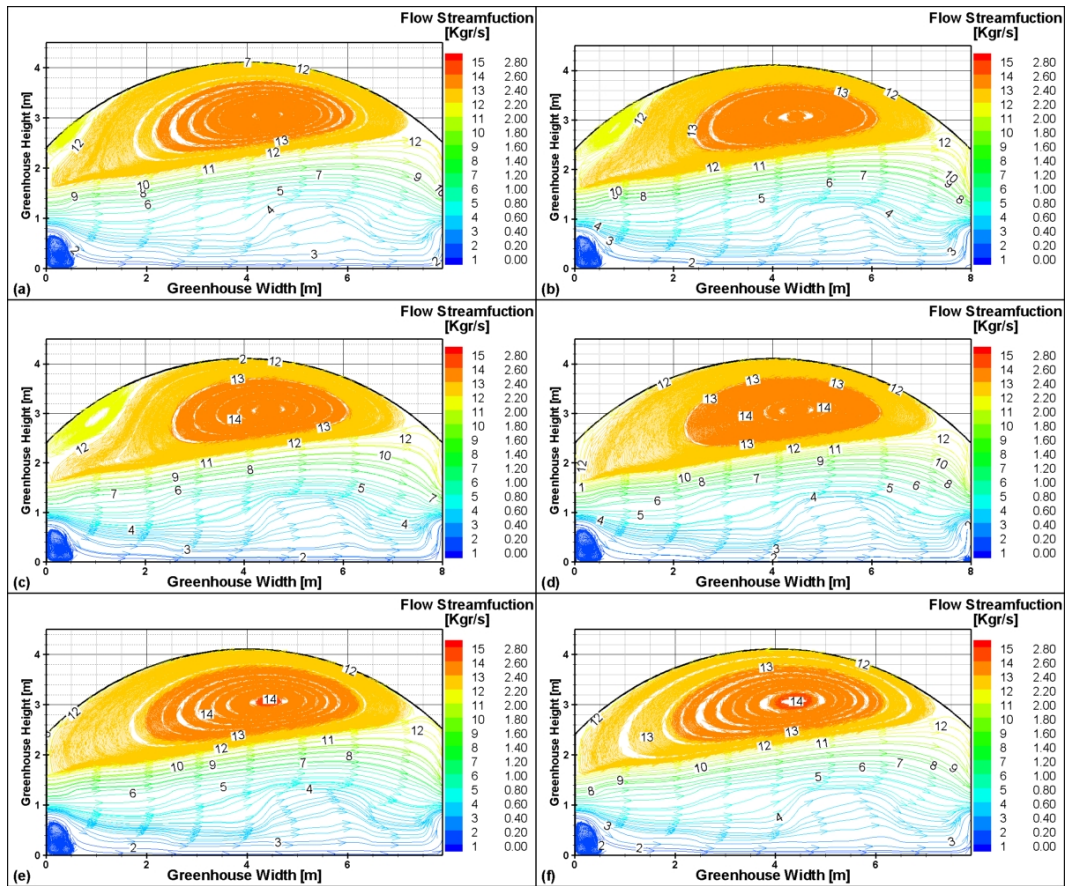
Figure 4 Streamlines of various inclinations of the incident solar radiation (a-e) and with no radiation effect (f): a) -60 degrees b) -30 degrees c) 0 degrees d) 30 degrees e) 60 degrees f) No radiation model applied

Figure 5 gives the u-velocity profiles at three positions inside the greenhouse at distances 2, 4 and 6 m from the inlet for all the five cases of Table 3. Close to the ground the velocity profile is almost identical for all cases characterised by an, almost rectangular, area of retardation caused by the resistance of tomato plants. The rectangular scheme fades close to the outlet. In the ground immediate vicinity, a small peak develops. However, the big peak appears just over the plants where the flow accelerates in order to transport a constant amount of flow through a narrow area. The peak position is elevated, while its magnitude is decreased from inlet to outlet, since the initial flow pattern is dissipated. Close to the cover, negative values of u-velocity appear since they correspond to big recirculation area.
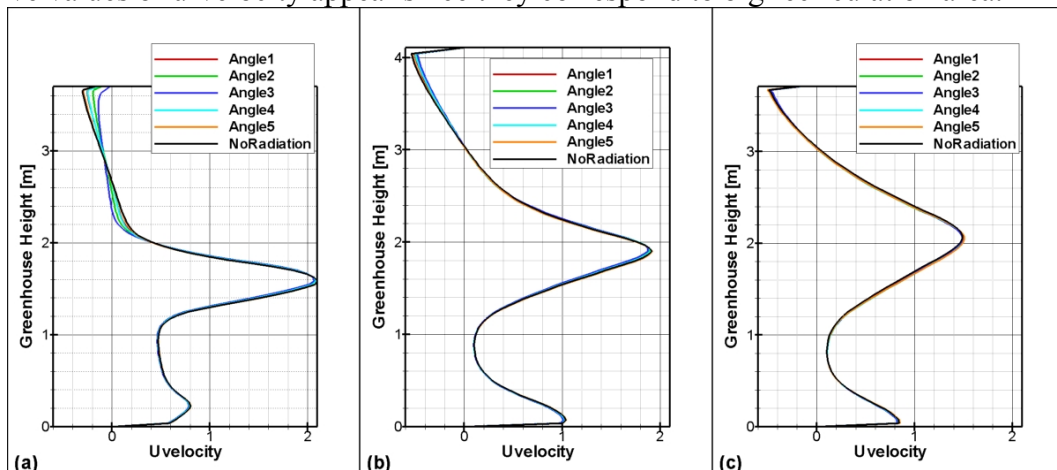

Figure 5: Profiles of U-velocity inside the greenhouse at 2m, 4m and 6m from the inlet

A slight differentiation of the profiles is observed in the upper part of the domain close to the inlet showing the dependence on hour angle. In this area the big recirculation is suppressed by the upper one during the early hours of the day till noon. It becomes apparent that apart from the fast moving inlet stream and the recirculation close to the roof, the buoyancy forces affect the flow as well.

3.1.2. Temperature variation

Figure 6 shows the air temperature distributions for the five cases of the hour angle parametric study (Table 3) plus the additional case where no radiation model applied.
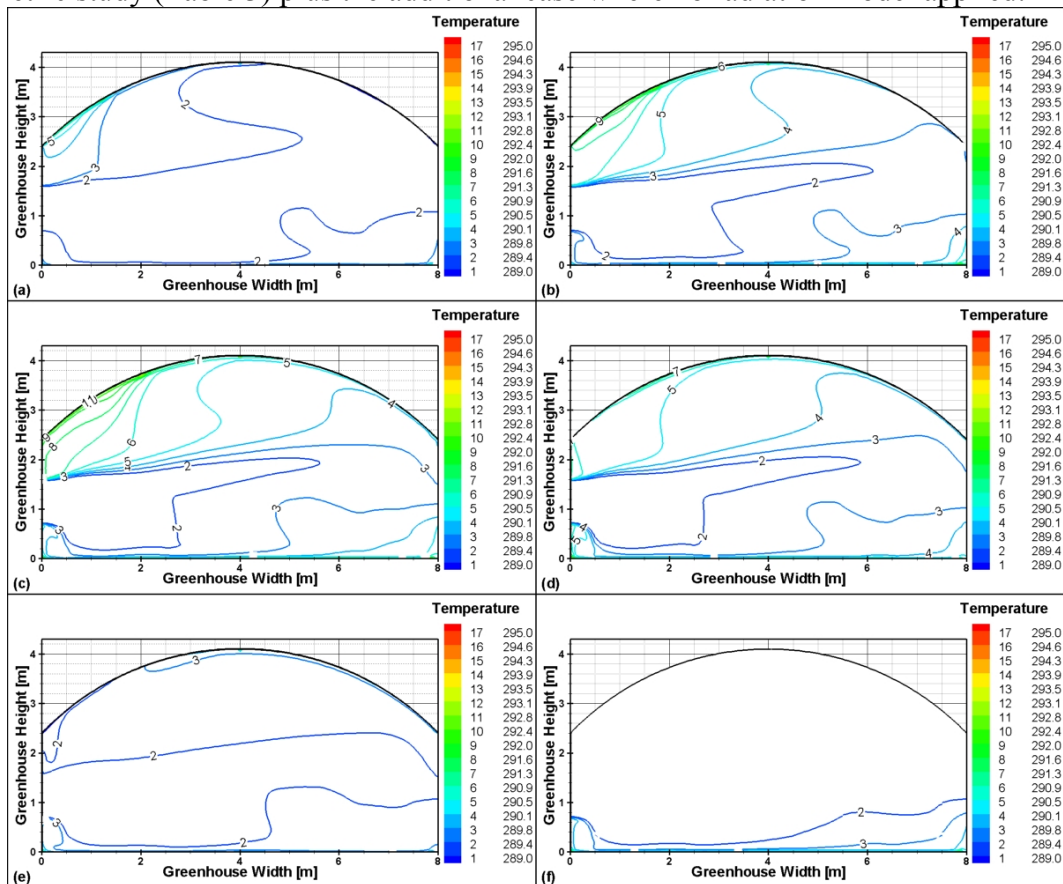

Figure 6 Temperature distributions for different inclinations of the incident solar radiation (a-e) and with no radiation effect (f): a) -60 degrees b) -30 degrees c) 0 degrees d) 30 degrees e) 60 degrees f) No radiation model applied

The main heat transfer mechanism is the forced convection. In the case (f), the temperature of the entering stream prevails in the whole domain, except from the area close to the ground and the bottom corners where the temperature is affected by the warmer ground, due to the reduced air velocity and to the recirculation. In cases (a) and (e), a core flow appears where the temperature of the entering stream remains unaffected. In cases (b), (c) and (d) the temperature in the core flow is affected by the combination of the UV and PAR solar radiation and the energy exchange with the plants (through radiation and convection). The effect of solar radiation in recirculation regions is more intensive resulting in a temperature rise and it is depended by hour angle. Cases with symmetric angle of incidence do not present similar distributions due to interaction of buoyancy forces with the entering stream.

Figure 7 presents the air temperature profiles for the same positions and cases described in Figure 5.
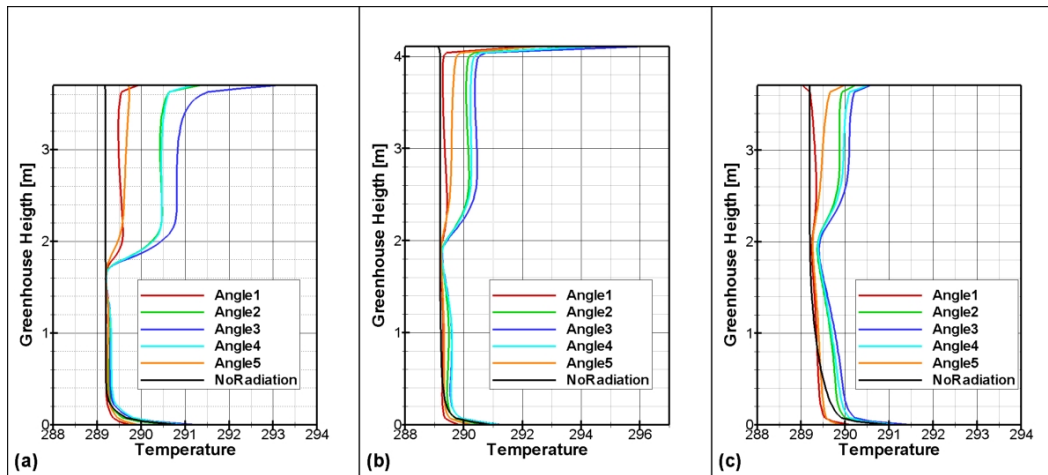
Figure 7 Temperature profiles inside the greenhouse at (a) 2m, (b) 4m and (c) 6m from the inlet

Two distinct areas can be observed: One in the bottom half domain, where the temperature distribution is mainly due to the entering stream temperature and the energy exchange with plants and another in the top half domain where the temperature is mainly affected by the incident radiation. Close to the inlet the two different domains behaves in extreme way, giving temperature differences of the order of 4 K in the upper half, while in the bottom one the temperature profile is totally independent on the angle of incidence. In the upper half of this region, symmetrical hour angles give similar temperature profiles with the $0°$ hour angle giving the higher air temperature. At the middle position the range of air temperature variation decreases and the rank of temperature profiles are determined by the hour angle. The temperature profile corresponding to the $0°$ hour angle gives the higher temperature followed by $+30°$, $-30°$, $+60°$ and $-60°$ hour angles. The last one gives a similar profile with the non-radiation case. The bottom half domain remains almost unaffected by the parameter of the hour angle. The temperature profiles corresponding near to the exit are ranked with the same order but in this case the variation range decreases further and is observed along the whole height of the section line. As the velocity of the entering stream reduces due to the plants' resistance, the mechanisms of energy exchange between air and plants are being more diffusive than convective.

3.1.3. Radiation distribution

Figure 8 presents the PAR contours for all cases of Table 3. The cover material allows the 83% of the incident radiation to be transmitted inside the greenhouse. Part of this is reflected by the plants (22%), resulting to a rise of the PAR intensity inside the structure and mainly close to the cover. However, at the interior of the greenhouse, the radiation intensity is reduced due to the indoor air which is supposed to have important absorptivity because of its water vapour content. In the crop zone, the PAR distribution is affected by the plants which absorb the PAR radiation, but they radiate at much higher wave lengths. The PAR intensity inside the greenhouse is the hour angle dependent and presents almost uniform distribution over the plants for the angles around the solar noon (Cases b,c and d). Nevertheless, in all cases the maximum PAR intensity is reaching roughly the same value proving the good functional performance of the arched design of the greenhouse's roof compared to other designs. Since the radiation transfer is independent of the flow field and the contribution of radiation from plants and greenhouses' materials is negligible for the PAR wavelength range, the symmetrical hour angles produce symmetrical PAR radiation patterns.
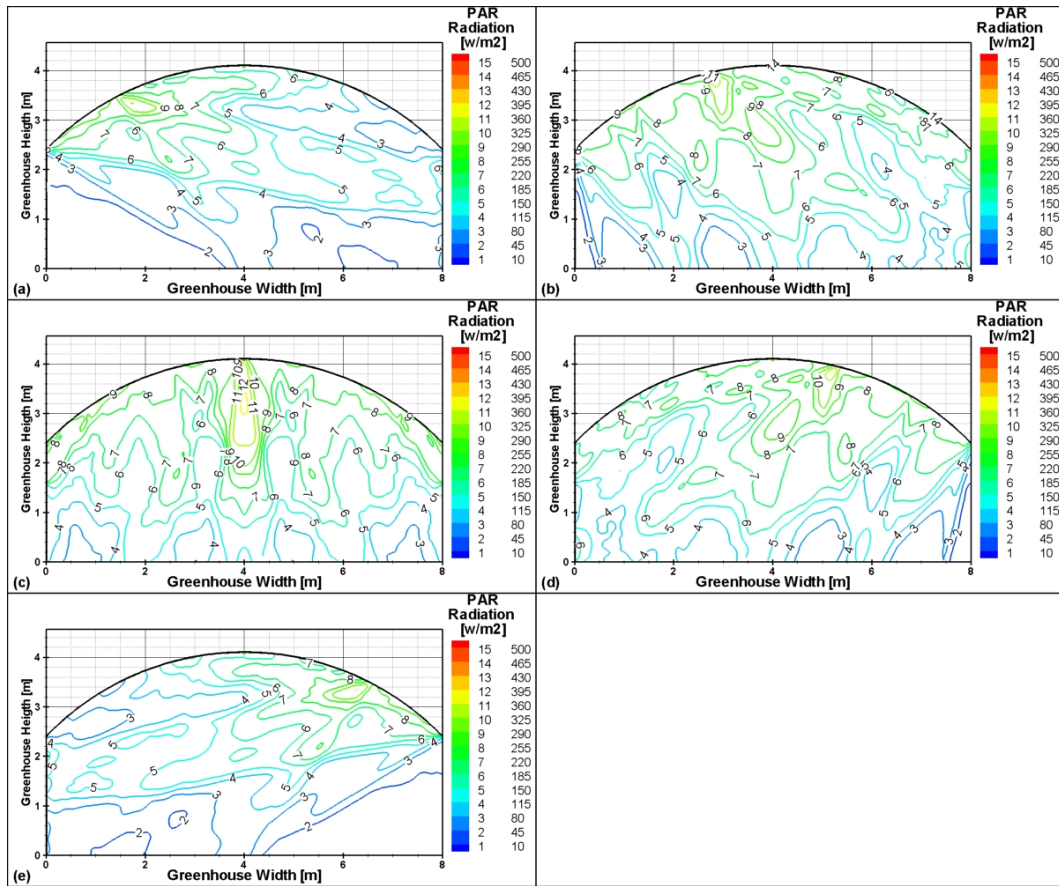
12

Figure 8 PAR distributions for different inclinations of the incident solar radiation (a-e) a) -60 degrees b) -30 degrees c) 0 degrees d) 30 degrees e) 60 degrees

Distributions of PAR along the greenhouse width at a height of 1 m from ground are presented in Figure 9. Full symmetry is verified along the greenhouse width for the studied cases. The plants' positions are recognised by the minima of the distributions, since they absorb radiation in order to photosynthesize. The available PAR intensity seems to be in same levels for the angles around the solar noon, and it is reduced to half for the cases which correspond to the morning and the afternoon. Plants located in the middle of the structure received higher amounts of PAR compared to those located near to greenhouse sides. This can lead to a totally different crop activities, and consequently, to a different crop growth and development.
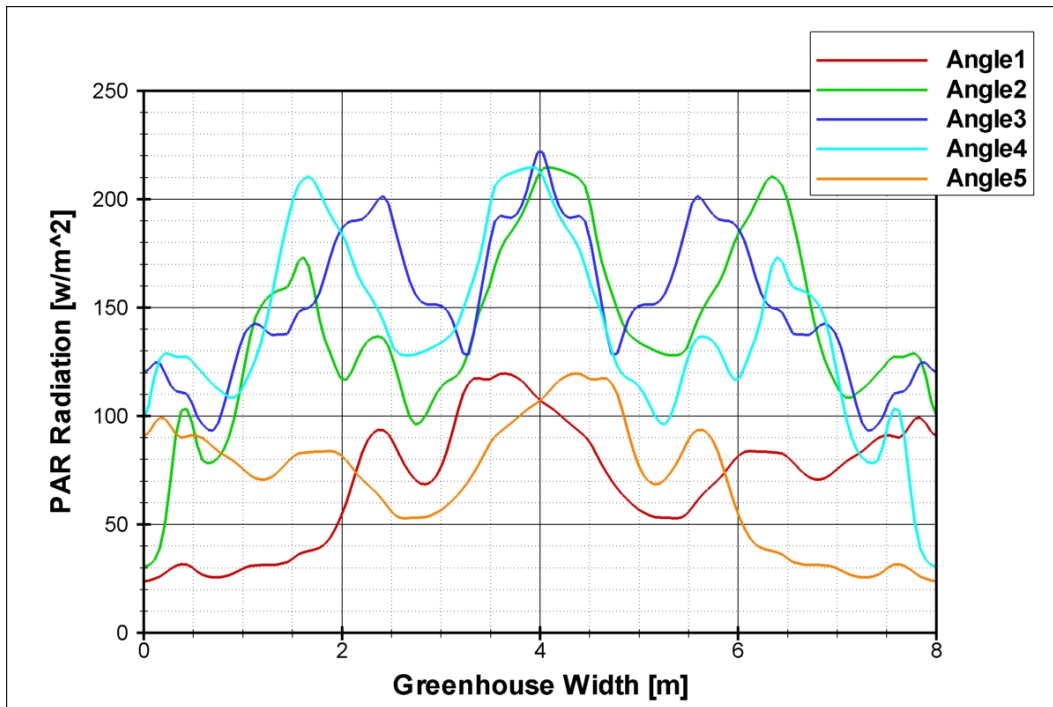
Figure 9 PAR profiles along greenhouse width at the level of 1m from greenhouse ground

3.1.4. Characteristic non-dimensional numbers

Figure 10 shows the radiation heat flux (a), the Nusselt number (b), the Boltzmann number (c) and the Stark number (d) along the internal side of the cover (Modest, 1993). In Table 5 the mean values of the above quantities are summarized.

The radiation heat flux integrated over all wavelength intervals is composed by the transmitted solar radiation, the radiation reflected by the structure and the plants and the long wavelength radiation emitted by the former parts. The results have symmetrical distributions. Hour angle 0° gives an almost perfect sinusoidal distribution with the higher peak value in the middle of the cover. Hour angles (+-)30° and (+-)60° give equally high peak values but they present points of discontinuity due to the cover geometry and the representation of the mesh boundary line with finite length rectilinear segments. The negative values denote heat transfer out of the domain mainly through emission of long wave radiation.

The dimensionless Nusselt number (Nu) expresses the ratio of convective to conductive heat transfer. On the contrary to latter quantity, the Nu number variations are not altered symmetrically. In addition, there are obvious discontinuities due to flow separation and reattachment on the greenhouse's cover and due to the temperature difference between the solid cover and the air. In general, the flow is highly convective with averages Nu number ranging from 250 close to sunrise and sunset and to 175 when the sun direction coincides with the entering stream allowing the development of the secondary recirculation in the inlet upper corner.
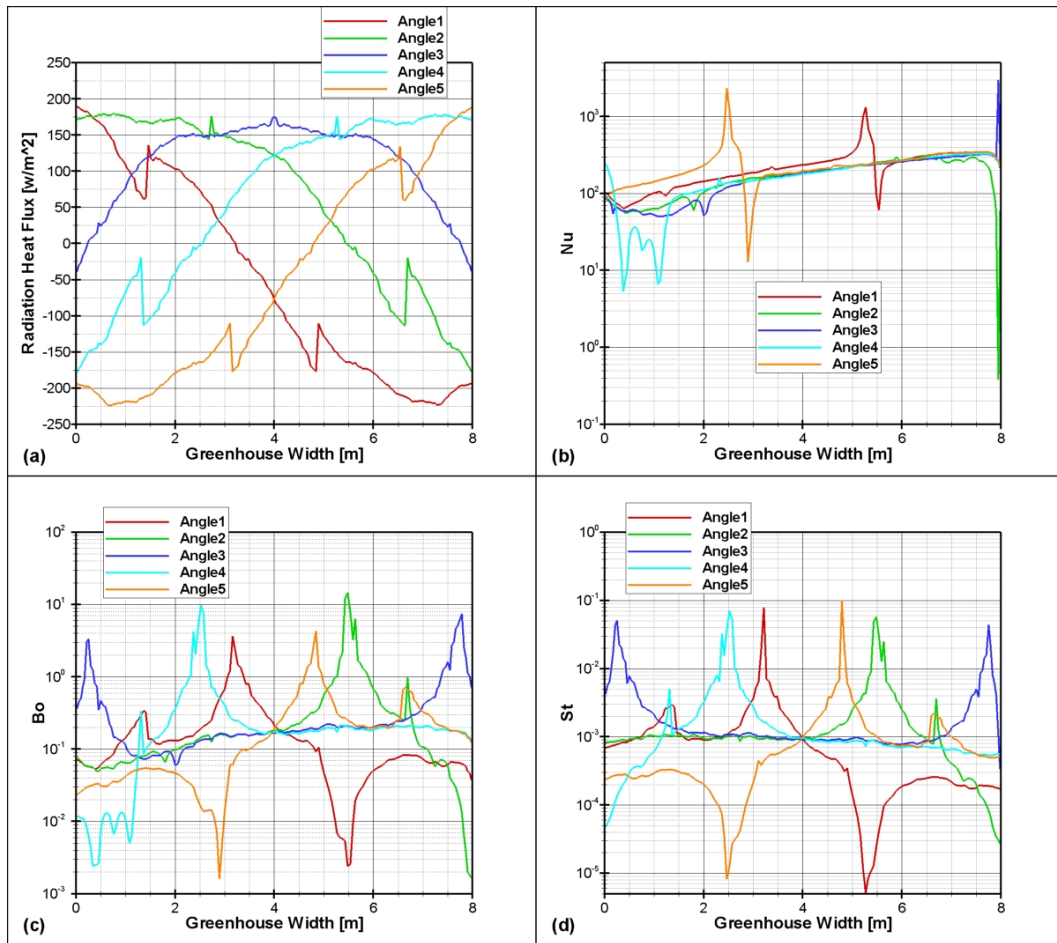
Figure 10 Radiation heat flux (a) Nusselt number (b) Boltzmann number (c) and Stark number (d) variation along the internal surface of the greenhouse cover for five hour angles

Table 5 First parametric study (hour angles) results

Case	Mean Radiation Heat flux [W/m^2]	Mean Nusselt Number [Nu]	Mean Boltzmann Number [Bo]	Mean Stark Number [N]
Angle -60	-48.405	233.26	0.198	0.0015
Angle -30	63.450	175.87	0.500	0.0022
Angle 0	107.497	195.79	0.515	0.0033
Angle +30	63.450	184.78	0.376	0.0025
Angle +60	-48.405	251.17	0.261	0.0015

The dimensionless Boltzmann number (Bo) expresses the ratio of convective to the radiative heat transfer. Here, the two heat transfer mechanisms seem to be comparable. In all cases the radiative heat flux predominates to the convective one but they both retain the same order. For hour angles where the secondary recirculation develops the Bo number denotes that the radiative heat transfer is twice the convective one while for the other cases the radiative heat transfer plays an even more important role. Hour angles (+-) 60° present a symmetrical behaviour.

The dimensionless Stark number (N) expresses the ratio of conductive to radiative heat transfer. From the specific graph, it derives that the conduction mechanism is not important.

15

Its value depends on the incident radiation the hour angle and the cover geometry and the distribution preserves noticeable symmetrical behaviour.

3.2 Influence of cover material

3.2.1. Flow field

Figure 11 presents the flow streamlines of all studied cases concerning the second parametric study (a-g) for the seven studied cover materials as they are described in Table 4. Different optical properties allow different amount of solar energy to enter the greenhouse, causing diversification in the flow pattern. This effect determines not only the size but even the existence of the upper corner recirculation. The materials are sorted in terms of recirculation size according to their absorptivity. The influence of this optical property to the development of the flow and thermal pattern inside the greenhouse will be further analyzed in the following paragraphs.
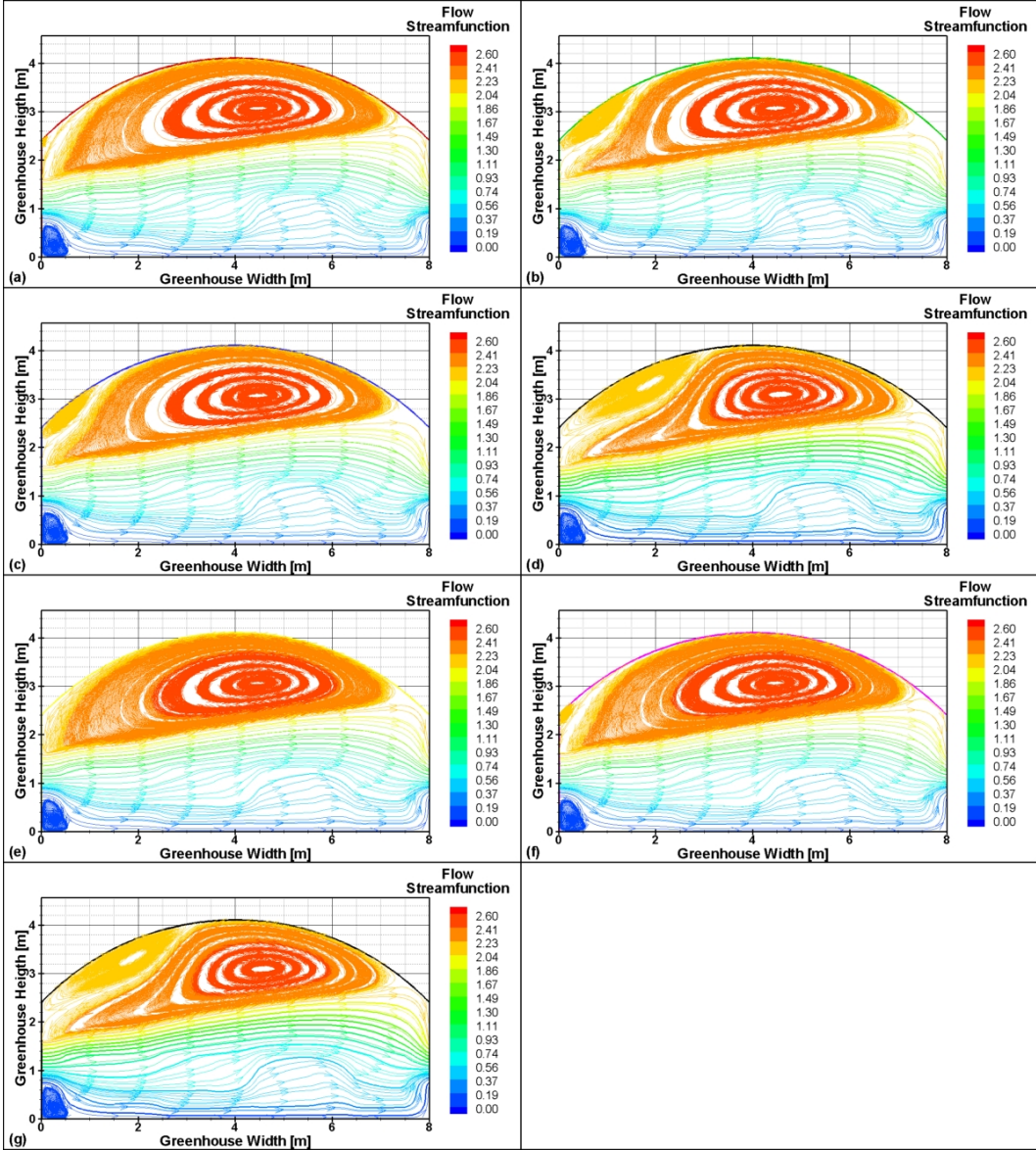

Figure 11 Streamlines for the seven different types of the covering materials (a-g) a) material 1, b) material 2, c) material 3, d) material 4, e) material 5, f) material 6 and g) material 7

The dependence of upper corner recirculation on the cover material is clearer in Figure 12 where the u-velocity profiles at the three positions inside the greenhouse at distances 2, 4 and 6 m from the inlet for all of the seven cases of Table 4 are presented. The diversification of the u-profile is restricted on the upper domain close to the inlet. From the other profiles it is concluded that the flow remains in the rest of the domain unaffected by the optical properties since the strong entering stream in combination with the plants' resistance prevail.
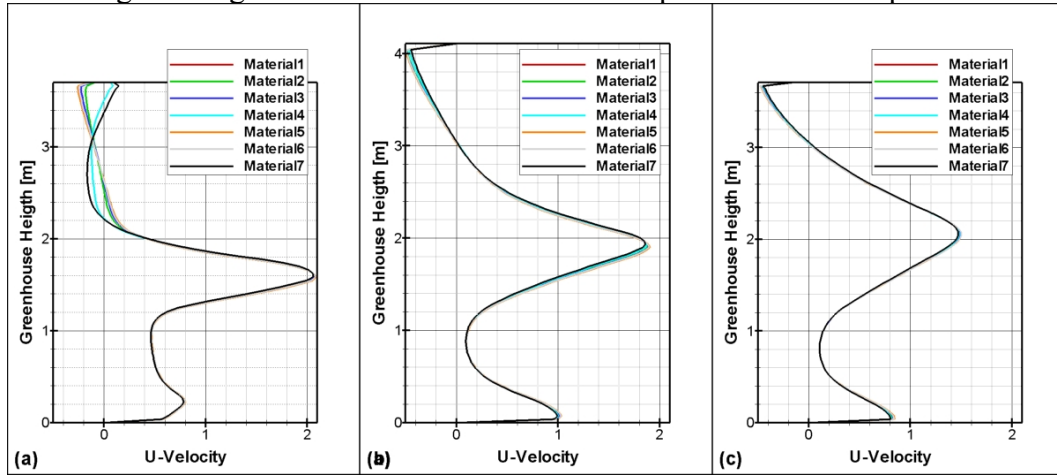
Figure 12 Profiles of U-velocity inside the greenhouse at 2m, 4m and 6m from the inlet for the second parametric study

3.2.2. Temperature variation

Figure 13 shows the temperature contours for the seven studied covering materials of Table 4. The main alterations on temperature distributions are marked out in the upper corner near the inlet since in this region the total heat transfer is stronger. The rest of the domain presents similar patterns for all examined cases. The extent of the later alterations is determined by two interactive feed backed mechanisms, while one enforces the other. For high absorptivity the cover temperature increases causing the heating by convection of the nearby air. The heated air causes local adverse pressure gradient resulting to flow separation, generating the upper corner recirculation. The temperature of the retarded air trapped in this recirculation increases further due to incoming transmitted radiation. The same behaviour is met in Figure 14 showing the temperature profiles at predefined positions.
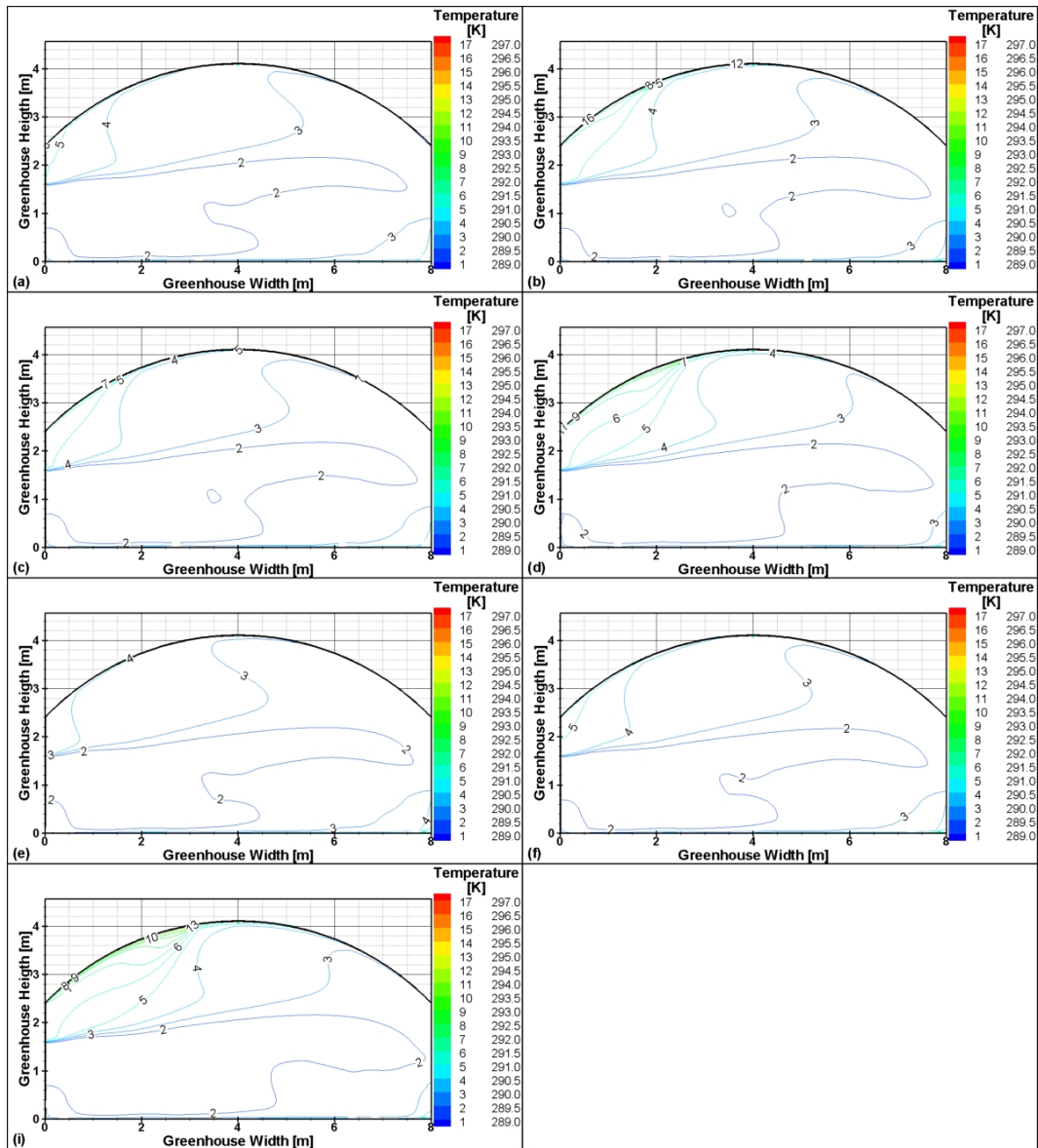
Figure 13 Temperature distributions inside of the greenhouse for the seven different types of
the covering materials (a-f) a) material 1, b) material 2, c) material 3, d) material 4,
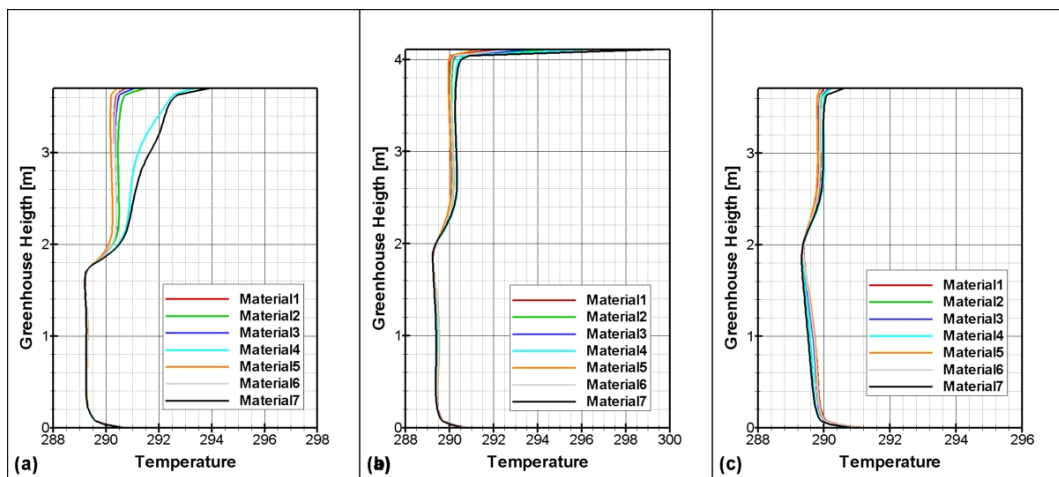e) material 5, f) material 6 and g) material 7

Figure 14 Temperature profiles inside the greenhouse at (a) 2m, (b) 4m and (c) 6m from the
inlet for the second parametric study

3.2.3. Radiation distribution

In Figure 15 the PAR radiation distribution isocontours are presented for the seven studied cover materials. The sort of materials in terms of inserted PAR into the interior greenhouse is defined according to materials transmittance. Material 7 with the lower transmittance allows small amount of PAR to enter the greenhouse while Material 5 with the higher transmittance allows higher amounts. The superiority of materials with high transmittance is also obvious from Figure 15 showing the distributions of available PAR along the greenhouse width at the level of 1 m from greenhouse ground. Observing the latter figure one may distinguish two group of material which present roughly similar behaviours. Materials 1, 2, 3, 5 and 6 have analogous performance while Materials 4 and 7 absorb significant amount of incident solar PAR, letting small percentage of it reach the crop level. The selection of Material 7 may reduce to a half the available PAR at the level of the crop inside the structure compared with Material 5.

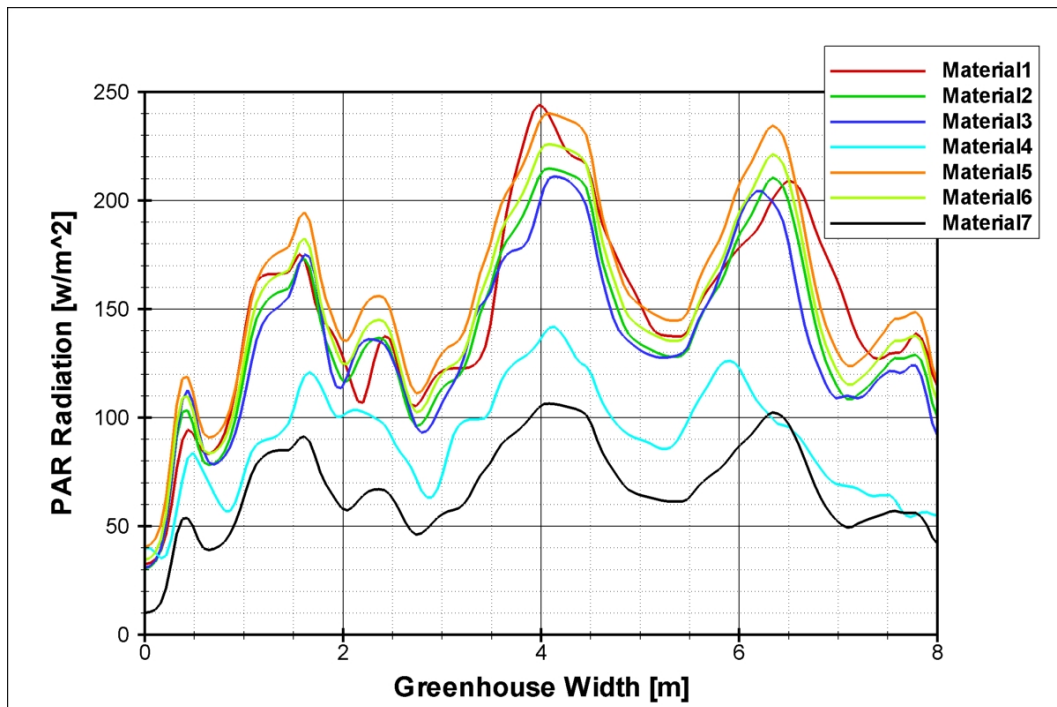Figure 15 PAR profiles along greenhouse width at the level of 1 m from greenhouse ground for the second parametric study

3.2.4. Characteristic non-dimensional numbers

Figure 16 shows the radiation heat flux (a), the Nusselt number (b), the Boltzmann number (c) and the Stark number (d) along the internal side of the cover for the second parametric study. Table 6 summarizes the mean values of the above quantities.
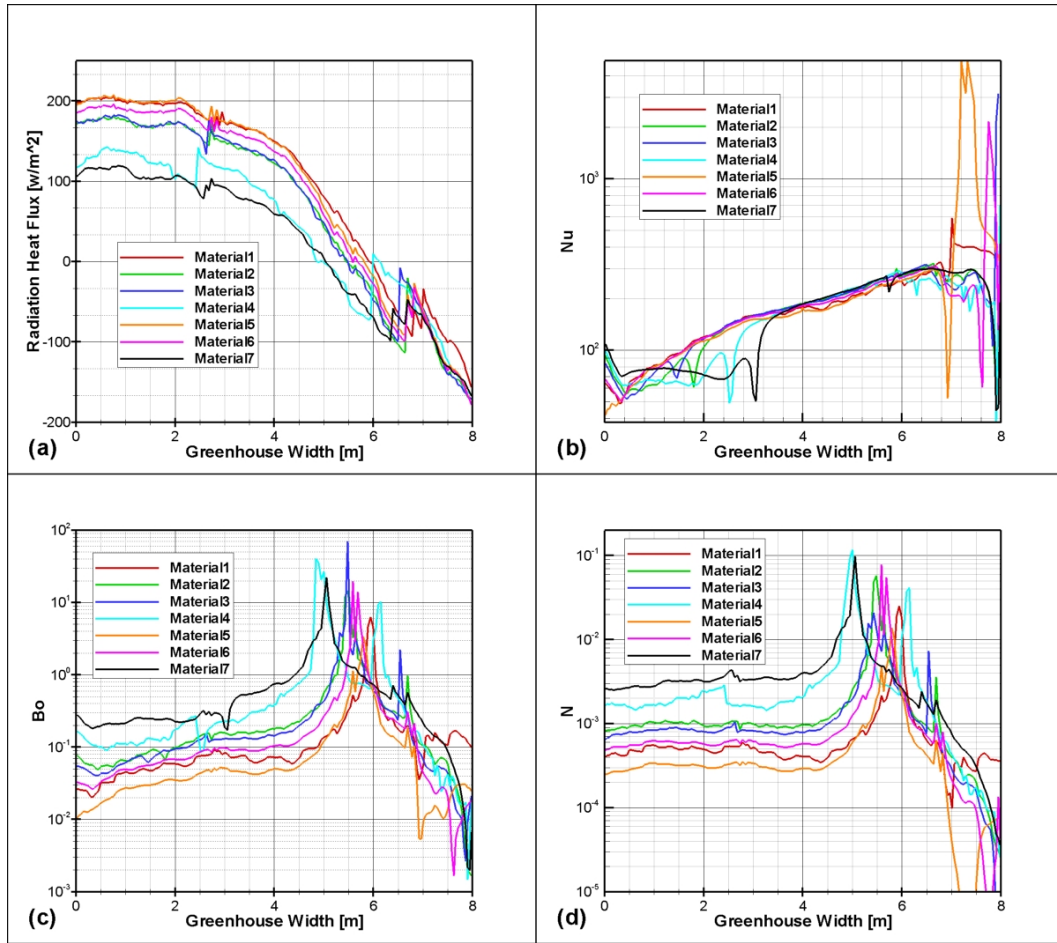
Figure 16 Radiation heat flux (a) Nusselt number (b) Boltzmann number (c) and Stark number (d) variation along the internal surface of the greenhouse cover for the seven studied materials

Table 6 Second parametric study (materials) results

Case	Mean Radiation Heat flux [W/m^2]	Mean Nusselt Number [Nu]	Mean Boltzmann Number [Bo]	Mean Stark Number [N]
Material 1	90.37	195.78	0.220	0.0011
Material 2	63.45	175.87	0.500	0.0022
Material 3	65.46	206.11	0.760	0.0016
Material 4	37.88	169.04	1.375	0.0055
Material 5	85.03	342.89	0.139	0.0006
Material 6	75.02	206.88	0.423	0.0018
Material 7	21.95	170.53	0.833	0.0045

Figure 16 (a) presents the radiation heat flux along the cover edge for all studied materials. As expected all distributions preserve almost the same patterns. Materials with high absorptivity (Material 5 & 7) permit lower radiative heat fluxes into the domain. Among the others, the higher radiative heat flux is observed for the material characterized by the lower refractive index (Material 1), although its absorptivity is relatively high.

Figure 16 (b) displays the variation of Nusselt number along the same edge as the previous figure (16 a). The local value of Nusselt number depends strongly on the existence of the secondary recirculation at the upper corner near the inlet. Small recirculation results to high velocities and consequently produces higher Nusselt numbers. Along the cover part

sided by the main recirculation, the Nusselt number follows similar trend for all cases showing that its evolution is independent by the optical properties of the covers and of the incident radiation heat flux. The last part near the corner over the exit presents extremely strong variations of heat conduction producing oscillations for the ratio of Nu number.

Finally Figures (16 c & 16 d) present the graphs of Boltzmann and Stark numbers along the cover line. Material with high absorptivity gives high Bo and N numbers. Materials with comparable absorptivity in terms of those dimensionless parameters are sorted according to their refractive indexes. Materials having high refractive index allow low radiation heat flux decreasing the denominator of ratios giving the Bo and N numbers.

4. Conclusions

The flow inside a greenhouse with continuous side vents along its length was simulated with a finite volume method, simulating the effect of external incident radiation with the DO model, distributed in three wavelength bands. Thermal and spectral optical properties both of covering materials and crop were taken into account, as well as the thickness of the cover material. The flow is dominated by three factors: (a) the strong entering stream from the leeward vent, (b) the plants which behave as porous obstacles and (c) one big recirculation close to the cover where the buoyancy forces, caused by the solar radiation, play an important role.

Although the main phenomenon is the entering stream, the whole flow pattern and the temperature distribution is significantly altered by the consideration of external incident radiation in the calculations. Two parametric studies were carried out in order to study the influence: a) of different radiation incident angle and intensity, and b) of cover materials with different optical properties. The results were presented in terms of velocity, temperature and PAR distributions and vertical profiles in characteristic positions inside the greenhouse, as well as in terms of radiation heat flux and dimensionless parameters along the cover.

Along the solar day the flow pattern varies as far is concern the appearance and the size of a secondary recirculation in the inlet upper corner. This recirculation from late morning (-30°) till the noon (0°) suppresses the big recirculation sited under the cover altering the mechanisms of heat transfer as denoted by the distribution of dimensionless numbers, Nu, Bo and N. In all cases the main mechanism of heat transfer through the cover is the radiation as it comes out from the values of Bo number, but convection also plays a significant role. From distribution of the PAR intensity at the level of the crop it is concluded that the plants close to the side receive noticeably lower amounts of PAR in comparison with plants sited in the middle, especially for the hour angles (+-60°) although the arching shape of the cover offer more uniform distribution during the rest of the solar day.

Cover materials with high absorptivity allow more significant local increase of air temperature inside the greenhouse favouring the development of secondary recirculation. But they result in low PAR intensity at the crop level. Among materials with comparable absorptpivity the more effective in terms of solar energy transfer are the ones which are characterized by low refractive index.

As over many years agricultural buildings have become tailored for specialised production, the need to maintain control over the indoor climate, so that the requirements of the production system can be continuously met, has become more important. Knowledge of the distribution of solar radiation inside greenhouses is of paramount importance in crop modelling studies especially in those aiming to assess the agronomic benefits of a given greenhouse cover material. The increasing interest in the use of photoselective covering materials in protected cultivations, together with new greenhouse types and ventilators systems, stresses the need to account for the cover radiation and thermal behaviour in greenhouse models in order to increase their accuracy and reliability in predicting canopy radiation absorption, and thus, crop photosynthesis and transpiration. The results of the

present study could be used for horticulturists to better understand and control greenhouse ventilation with respect to crop activity, for the growers in tuning their irrigation and shading scheduling, for plastic industries as a basic tool for future improvements in their covering materials, and finally for greenhouse manufacturers to improve greenhouse designs and to adapt the greenhouse equipment to specific cases.

Nomenclature

a   porous permeability [m^2]

Bo   Boltzmann number [-] (Bo=convection/radiation) $Bo = \dfrac{\rho\, C_P\, u_\infty}{n^2\, \sigma\, T_\infty^3}$

C$_2$ inertial resistance factor [1/m]
C$_p$ specific heat capacity [J/(kg K)]
d   thickness [m]
f$_b$ buoyancy force [N/m^3]
h   sensible enthalpy [J/Kg], convective heat transfer coefficient [W/m^{2}K]
I   radiation intensity [W/m^2]
I$_\lambda$ radiation intensity for wavelength λ [W/(m^2 sr)]
I$_{b\lambda}$ black body intensity given by the Planck function [W/m^2]
k   turbulent kinetic energy [J/kg], Thermal conductivity [W/(m K)]
k$_{eff}$ effective conductivity [W/(m K)]
L   characteristic length [m]
n   refractive index of medium b [-]

N   Stark number [-] (N=conduction/radiation) $N = \dfrac{k\, \alpha_\lambda}{4\, n^2 \sigma T_\infty^3}$

Nu   Nusselt number [-] (Nu=convection/conduction) $Nu = \dfrac{h\, L}{k}$

P   pressure [Pa]
$\vec{r}$ position vector [-]
S$_i$:   momentum source term due to presence of porous media [J]
S$_h$ radiation source term [J]
$\vec{s}$ radiation direction vector [-]
$\vec{s'}$ scattering direction vector [-]
T$_\infty$ free stream temperature [K]
T   temperature
U$_i$ average velocity in i-direction [m/s]
x$_i$ component in i-direction [m]

Greek Letters
α absorptivity (or absorptance) [-]
α_λ spectral absorption coefficient or extinction coefficient [1/m]
ε turbulent dissipation rate [J/(Kg s)], emissivity [-]
λ wavelength [m^{-1}]
μ viscosity [Pa sec]
μ_t turbulent viscosity [Pa sec]
ρ density [kg/m^3]
σ_s scattering coefficient [1/m]
Φ phase function [-]
Ω' solid angle [deg]

References

Bartzanas, T., T. Boulard and C. Kittas. 2004. Effect of vent arrangement on windward ventilation of a tunnel greenhouse. Biosystems Engineering, 88: 479-490.

Bot G. P. A. 2001. Developments in indoor sustainable plant production with emphasis on energy saving. Computers and Electronics in Agriculture, 30: 151-165.

Boulard T. and S. Wang. 2002. Experimental and numerical studies on the heterogeneity of crop transpiration in a plastic tunnel. Computers and Electronics in Agriculture, 34: 173-190.

Chui, E. H. and G. D. Raithby. 1993. Computation of radiant heat transfer on a nonorthogonal mesh using the finite-volume method. Numerical Heat Transfer. Part B, Fundamentals, 23: 269-288.

Cockshull, K. E., C. J. Graves and R. J. Cave. 1992. The influence of shading on yield of glasshouse tomatoes. Journal of Horticultural Science, 67: 11-24.

Critten, D. L. 1993. A review of the light transmission into greenhouse crops. Acta Horticulturae, 328: 9-32.

De Tourdonnet, S. 1998. Maîtrise de la qualité et de la pollution nitrique en production de laitues sous abris plastique: diagnostique et modélisation des effets des systèmes de cultureThèse de Doctorat l'INRA Paris-Grignon.

De Zwart, H. F. 1993. Determination of Direct Transmission of a Multispan Greenhouse Using Vector Algebra. Journal of Agricultural Engineering Research 56: 39-49.

Deshpande, M. D. and D. P. Giddens. 1980. Turbulence measurements in a constricted tube. Journal of Fluid Mechanics, 97: 65-89.

Duffie, J. A. and W. A. Beckman. 1980. Solar Engineering of Thermal Processes, 2nd edn. Willey Interscience, New York.

Fatnassi, H., T. Boulard, C. Poncet and M. Chave. 2006. Optimisation of greenhouse insect screening with computational fluid dynamics. Biosystems Engineering, 93: 301-312.

Ferziger, J. H. and M. Peric. 2002. Computational methods for fluid dynamics. Springer, London.

Fluent. 1998. FLUENT v5.3 Manual, Sheffield, UK.

Gray D. D. and A. Giorgini. 1976. The validity of the Boussinesq approximation for liquids and gases. International Journal of Heat and Mass Transfer, 19: 545-551.

Kim, S. H. and K. Y. Huh. 1999. A new angular discretization scheme of the finite volume method for 3-D radiative heat transfer in absorbing, emitting and anisotropically scattering media. International Journal of Heat and Mass Transfer, 43: 1233-1242.

Kittas, C. and A. Baille. 1998. Determination of the spectral properties of several greenhouse cover materials and evaluation of specific parameters related to plant response. Journal of Agricultural Engineering Research, 71: 193-202.

Kurata, K. 1990. Role of reflection in light transmissivity of greenhouses. Agricultural and Forest Meteorology, 52: 319-331.

Kurata, K., Z. Quan and O. Nunomura. 1991. Optimal shapes of parallel east-west oriented single span tunnels with respect to direct light transmissivity. Journal of Agriculture Engineering Research, 48: 89-100.

Launder, B. E. and D. B. Spalding. 1972. Lectures in mathematical models of Turbulence. Academic Press, London, England.

Modest, M. M. 1993. Radiative Heat Transfer, 1st edn. McGraw Hill International Ed., Singapore.

Mohammadi, B. and O. Pironneau. 1994. Analysis of the k-epsilon Turbulence Model. Research in Applied Mathematics. Wiley, New York, Masson, Paris.

Molina-Aiz, F. D., D. L. Valera, A. J. Alvarez and A. Maduen. 2006. A wind tunnel study of airflow through horticultural crops: determination of the drag coefficient. Biosystems Engineering, 93: 447-457.

Monteith J. L. 1973. Principles of environmental Physics. Contemporary Biology, Edward Arnold, London, UK, 241 pp.

Monteith, J. R. 1977. Climate and the efficiency of crop production in Britain. Philosophical Transactions of the Royal Society of London, Series B, 281: 277-294.

Murthy, J. Y. and S. R. Mathur. 1998. Finite volume method for radiative heat transfer using unstructured meshes. Journal of Thermophysics and Heat Transfer, 12: 313-321.

Ould Khaoua, S. A., P. E. Bournet, C. Migeon, T. Boulard and T. Chasseriaux. 2006. Analysis of greenhouse ventilation efficiency based on computational fluid dynamics. Biosystems Engineering, 95: 83-98.

Papadakis, G., D. Manolakos and S. Kyritsis. 1998. Solar radiation transmissivity of a single span greenhouse through measurements on scale models. Journal of Agricultural Engineering Research, 71: 331-338.

Patankar, S. V. 1980. Numerical heat transfer and fluid flow. Hemisphere, Washington, D.C.

Pieters, J. G. and J. M. Deltour. 1997. Performances of Greenhouses with the Presence of Condensation on Cladding Materials. Journal of Agricultural Engineering Research, 68: 125-137.

Pollet, I. V., F. P. Thoen and J. G. Pieters. 1999. Solar energy availability in greenhouses as affected by condensation on cladding materials. Renewable Energy, 16: 769-772.

Raithby, G. D. 1999. Discussion of the finite-volume method for radiation, and its application using 3D unstructured meshes. Numerical Heat Transfer, Part B: Fundamentals, 35(4): 389 - 405.

Raithby, G. D. and E. H. Chui. 1990. A Finite-Volume Method for Predicting a Radiant Heat Transfer in Enclosures with Participating Media. Transactions of ASME Journal of Heat Transfer, 112: 415-423.

Rosa, R., A. M. Silva and A. Miguel. 1989. Solar irradiation inside a single-span greenhouse. Journal of Agricultural Engineering Research, 43: 221-229.

Takakura, T. 1993. Climate under cover-digital dynamic simulation in plant bio-engineering. Kluwer Academic Press, Netherlands.

Tamamidis, P. and D. N. Assanis. 1993. Evaluation of various high order accuracy schemes with and without flux limiters. International Journal for Numerical Methods in Fluids, 16: 931-948.

Vougioukas, S. 2004. Multi-spectrum Global Illumination Computation For Greenhouse Applications. In: 2nd HAICTA International Conference on Information Systems & Innovative Technologies in Agriculture, Food and Environment., Thessaloniki, Greece, pp. 47-56.

Wang, S. and T. Boulard. 2000. Measurement and prediction of solar radiation distribution in full-scale greenhouse tunnels. Agronomie, 20: 41-50.